# Fragmentation Dynamics in Equity Markets During Global Crises

Laura Molero González [1,2], Antonio M. Puertas [3], Juan E. Trinidad Segovia[4], Miguel A. Sánchez Granero [5]

[1,4] Department of Economics and Business, University of Almería, 04120, Almería, Spain.
[2] Department of Social and Economic Sciences, Sapienza University of Rome, 00185, Rome, Italy.
[3] Department of Physics, University of Almería, 04120, Almería, Spain.
[5] Department of Mathematics, University of Almería, 04120, Almería, Spain.

**Email:** lmg172@ual.es (L. Molero González); apuertas@ual.es (A. M. Puertas); jetrini@ual.es (J. E. Trinidad Segovia); misanche@ual.es (M.A. Sánchez Granero)

**Abstract**

This paper aims to study how different types of crises affect the dynamics of financial markets through the lens of cross-sectional fragmentation. We employ a measure of dynamical susceptibility from statistical physics to capture the degree of heterogeneity in asset price dynamics across markets. Using daily data from 12 developed and emerging equity markets over the period 2005–2026, we show that financial crises, pandemics, and geopolitical shocks generate distinct fragmentation signatures.

Our results indicate that the 2008 financial crisis led to a globally synchronized increase in market fragmentation, consistent with a systemic breakdown. In contrast, the Covid-19 pandemic produced a sharper and more pervasive disruption, particularly affecting developed markets. Meanwhile, the Russia–Ukraine war exhibited a localized impact, primarily concentrated in European markets. Moreover, the rolling-window analysis performed reveals that increases in fragmentation often precede peak stress periods, suggesting that this measure is able to capture the build-up of dynamical instability.

These findings highlight that market instability is not a one-dimensional phenomenon and that different shocks induce fundamentally different responses across financial systems.

**Keywords:** Market fragmentation, systemic risk, dynamical susceptibility, economic crises.

## 1 Introduction

The concept of dynamical susceptibility is borrowed from statistical physics, where it indicates how sensitive a system is to an external stimulus. Whereas the susceptibility has been long used in different fields of physics, such as electromagnetism or thermodynamics, to measure, e.g. the electric response of a system, the dynamical susceptibility has been introduced recently to study complex fluids in soft matter, close to the glass transition. There, important dynamical heterogeneities were observed, without concomitant structural inhomogeneities. The dynamical susceptibility is calculated as the variance of the density autocorrelation function, based on linear response theory, which assumes that a system will recover from an external stimulus similar to its internal fluctuations in equilibrium, i.e., without external force.

In this paper, we focus on cross-sectional fragmentation as a key dimension of market instability. We argue that different types of crises not only differ in magnitude, but also in the structural way in which markets become disorganised. In this context, we employ a measure of dynamical susceptibility that allows us to identify distinct fragmentation signatures associated with financial, biological, and geopolitical shocks.

Our contribution is threefold. First, we adapt and implement a measure of dynamical susceptibility, originally developed in the context of econophysics, to capture market fragmentation in a financial setting.

Second, we provide empirical evidence that different types of crises generate distinct structural responses in financial markets, which we characterise as "fragmentation signatures". Third, we show that the temporal evolution of fragmentation contains early signals of market stress that are not fully captured by traditional indicators.

The rest of the paper is organised as follows: Section 2 presents the dataset analysed in this study, jointly with the main methodological instruments employed and the description of the empirical experiment performed, Section 3 presents and discusses the results, and Section 4 concludes.

# 2 Materials and methods

## 2.1 Data

To achieve the objectives of this study, we analyze the daily closing prices of stocks from 12 distinct financial markets, comprising five developed and seven emerging economies. The developed markets include the S&P 500 (USA), FTSE 100 (UK), CAC 40 (France), DAX 40 (Germany), and FTSE MIB (Italy). The emerging markets group consists of Ibovespa (Brazil), SSE 50 (China), S&P CLX IPSA (Chile), BSE SENSEX (India), KOSPI (South Korea), ATHEX Composite (Greece), and TWSE (Taiwan).

The study period ranges from January 1st, 2005, to March 30th, 2026. Due to the different scales of nominal stock prices across countries, the analysis is conducted using the natural logarithms of the closing prices. The slight discrepancies in the number of observations ($n$) between indices reflect the asynchronous nature of global trading calendars and local public holidays, ensuring that only active trading sessions are considered for each specific market.

To ensure data quality, we applied a rigorous cleaning procedure: only stocks with less than 5% of missing trading days over the entire period were considered, while those failing to meet this threshold were excluded. For the remaining assets, linear interpolation was used for gaps smaller than three consecutive days. The final number of companies ($p$) retained for each market and the main descriptive statistics for the log-transformed prices are reported in Table 2 in Appendix A.

## 2.2 Methodology

### 2.2.1 Measures of Dynamic Heterogeneity in Stock Markets

In order to characterise the dynamical properties of financial markets, we adopt a framework inspired by the physics of glass-forming systems. Following Molero-González et al. (2025), we interpret the logarithm of stock prices as the analogue of particle positions in a many-body system. Thus, for each asset $j$, we define $x_j(t) = \log P_j(t)$.

To quantify the temporal evolution of price fluctuations, we compute the overlap function, defined as in (2).

$$\Phi_\Delta(t,\tau) = \frac{1}{p}\sum_j \theta(|x_j(t+\tau) - x_j(t)| - \Delta), \tag{1}$$

$$\Phi_\Delta(\tau) = \langle \Phi_\Delta(t,\tau) \rangle \tag{2}$$

where $\theta(\cdot)$ denotes the Heaviside function, $p$ is the number of assets in the market, $\Delta$ represents a threshold for price variation, and $\langle\cdot\rangle$ indicates averaging over time origins $t$.

This function is an approximation of the self-intermediate scattering function, sISF, used in complex fluids to characterise the dynamical susceptibility. The sISF measures the decorrelation of a system from its initial configuration, and is calculated as the Fourier transform of the mean squared displacement, whereas the current function, $\Phi_\Delta$, also gives the same information and is easily calculated. Furthermore, it can be directly interpreted in financial markets as the fraction of assets whose log-price variation remains below a given threshold $\Delta$ over a time lag $\tau$, thereby capturing the occurrence of significant price adjustments across assets. Different values of $\Delta$ are considered in order to probe the relaxation dynamics at multiple fluctuation scales; concretely, we perform the analysis for $\Delta \in \{0.02, 0.04, 0.06, 0.08\ldots, 0.20\}$.

The choice of these values for the parameter $\Delta$ is motivated by their financial interpretation, as they correspond to log-price variations ranging from 2% to 20%. This range allows us to explore the market's response to both typical daily fluctuations and more extreme price adjustments that occur during periods of financial distress.

To further analyse dynamical heterogeneities, we compute the dynamical susceptibility associated with the overlap function, defined in (3) as the variance of $\Phi_\Delta(\tau)$:

$$\chi_\Delta(\tau) = \left\langle \Phi_\Delta(t,\tau)^2 \right\rangle - \left\langle \Phi_\Delta(t,\tau) \right\rangle^2 . \tag{3}$$

This quantity captures fluctuations in the relaxation dynamics and serves as an indicator of dynamical heterogeneity in the system. In particular, the presence of a peak in $\chi_\Delta(\tau)$ indicates that different assets adjust over distinct time scales, reflecting a lack of synchronisation in their dynamics.

From a financial perspective, $\chi_\Delta(\tau)$ can be interpreted as a measure of cross-sectional instability. While standard indicators such as volatility capture the magnitude of aggregate fluctuations, and correlation-based measures capture co-movement, $\chi_\Delta(\tau)$ reflects the degree of synchronisation in the adjustment process across assets. High values indicate that assets do not adjust synchronously to market conditions, leading to a fragmented market structure where different groups of stocks evolve at different speeds. In this sense, $\chi_\Delta(\tau)$ does not only reflect the magnitude of price fluctuations, but rather the degree of coordination in market dynamics. Elevated values indicate that the market is no longer evolving as a coherent system, but instead displays fragmented behaviour across groups of assets. This fragmentation is particularly relevant during periods of market stress, when the stability of correlation structures and the effectiveness of diversification may deteriorate. In this context, $\chi_\Delta(\tau)$ provides a complementary perspective on market instability by capturing the dispersion in dynamic responses rather than the magnitude of price movements alone.

#### 2.2.2 Event-Based Analysis and Longitudinal Market Monitoring

To assess the evolution of dynamical heterogeneities over time and the market response to major global shocks, we adopt two complementary analysis schemes. First, we implement with a static event window approach. We analyse specific periods associated with major financial and geopolitical crises to assess how market stability and heterogeneity evolve across different phases of each event. Specifically, we define windows for (a) the global financial crisis (2007–2009), (b) the European debt crisis (2011–2012), (c) the Covid-19 pandemic crisis (2020–2021), and (d) the Russia-Ukraine war conflict (2022). Each event is divided into pre-crisis, crisis, and post-crisis stages to identify shifts in market stability and heterogeneity as presented in Table 1. We acknowledge that some periods overlap due to the sequential nature of these global shocks, where the aftermath of one crisis frequently bleeds into the early stages of the following one.

Table 1: Temporal segmentation of the four major economic and geopolitical shocks studied.

| | Global Financial Crisis | European Debt Crisis | Covid-19 Pandemic Crisis | Russia-Ukraine War Conflict |
|---|---|---|---|---|
| Pre-crisis | 01/01/2005 – 30/07/2007 | 01/01/2009 – 31/12/2010 | 01/01/2018 – 28/02/2020 | 01/01/2021 – 31/12/2021 |
| Crisis | 01/08/2007 – 31/12/2009 | 01/01/2011 – 31/12/2012 | 01/03/2020 – 31/12/2021 | 01/01/2022 – 31/12/2022 |
| Post-crisis | 01/01/2010 – 31/12/2011 | 01/01/2013 – 31/12/2014 | 01/01/2022 – 31/12/2023 | 01/01/2023 – 31/12/2024 |

Furthermore, we implement a rolling window analysis with the aim of capturing the continuous evolution of the market dynamics. We use a fixed window size of $W = 252$ trading days (equivalent to approximately one trading year), which shifts with a step of $S = 5$ days. For each window, the correlation function $\Phi_\Delta(\tau)$ and the susceptibility $\chi_\Delta(\tau)$ are recalculated. This provides a time-resolved view of the dynamical parameters, allowing us to identify early signals of market fragmentation and potential precursors of financial instability.

These calculations are performed not only for each market but also by aggregating assets into broader categories. Specifically, we group the indices based on their geographical region (America, Asia, and Europe) and their level of economic development (developed and emerging markets).

# 3 Results and discussion

This section is devoted to the presentation of the results obtained in this study. To characterise the dynamic heterogeneity of financial markets during periods of stability and stress, we first examine the behaviour of the dynamic susceptibility $\chi_\Delta(\tau)$ across the entire market sample. The curves displayed in Figure 1 reveal a universal feature: for each market index and across all price variation thresholds, the susceptibility exhibits a pronounced maximum at a specific time lag $\tau_m$, indicating that different assets adjust their positions over distinct time scales. The position and magnitude of this maximum are not fixed but instead shift as a function of the threshold parameter $\Delta$, reflecting the market's differential response to price movements of varying magnitudes. To understand how financial crises disrupt this structure, we proceed to analyse the evolution of $\mathrm{Max}(\chi_\Delta)$ and the corresponding characteristic times, $\tau_m$, across the pre-crisis, crisis, and post-crisis periods of four major economic shocks.

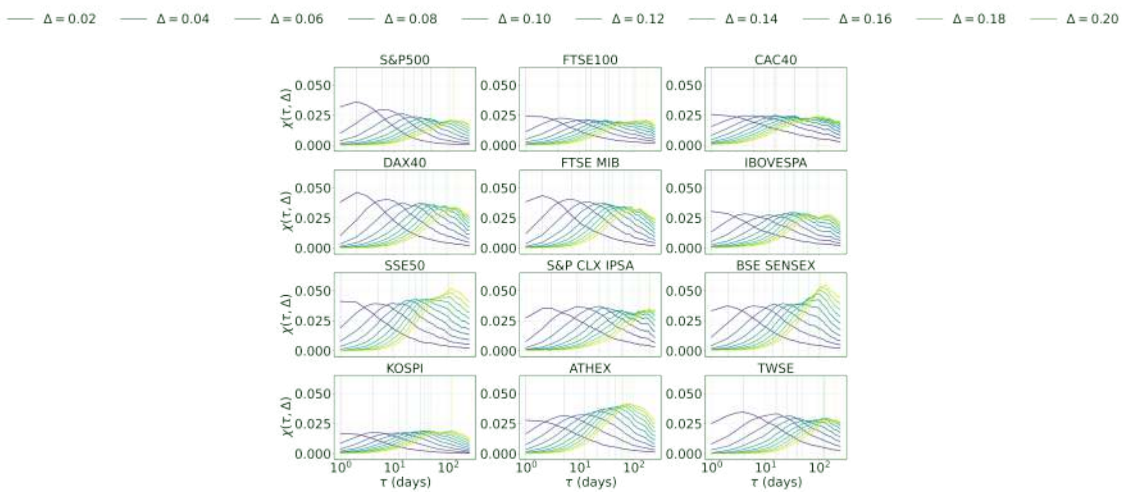


Figure 1: Dynamic susceptibility $\chi_\Delta(\tau)$ as a function of time lag $\tau$ for twelve global equity market indices across different price variation thresholds $\Delta \in [0.02, 0.20]$. Each panel represents a distinct market index, with colored curves corresponding to different $\Delta$ values. All curves exhibit a characteristic maximum at specific time scales, indicating the presence of distinct adjustment dynamics across markets and the lack of synchronisation in cross-sectional price movements at different frequency levels.

As a preliminary step, we assessed whether $\mathrm{Max}(\chi_\Delta)$ is able to provide additional information relative to standard financial indicators. To this end, we benchmarked its performance across all markets against realised volatility and pairwise correlations. In this way, while $\mathrm{Max}(\chi_\Delta)$ tends to increase during periods of market turmoil, its correlation with the analysed traditional indicators varies significantly from one market to another. This result suggests that the considered measure is able to capture additional dimensions of market instability, concretely, the degree of synchronisation in the adjustment process across assets. All these preliminary results are reported in the Appendix C

Then, we continued with the characterisation of the intensity of market heterogeneity during the four major global events selected for this study: the 2008 financial crisis, the European debt crisis, the Covid-19 pandemic, and the Russia-Ukraine war. We quantify this intensity through the maximum dynamic susceptibility ($\mathrm{Max}(\chi_\Delta)$, hereinafter), which identifies the point of greatest structural divergence in each market.

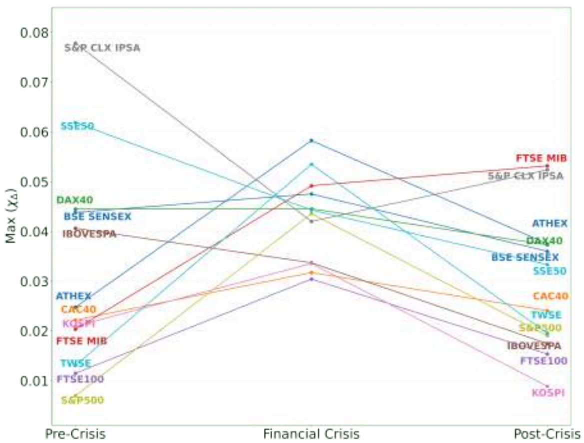


(a) 2008 Global Financial Crisis

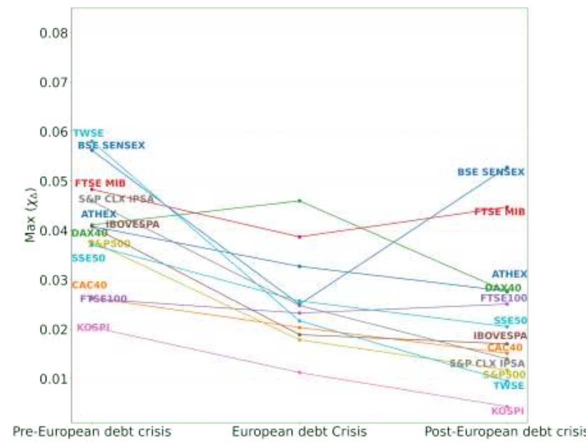


(b) European Debt Crisis

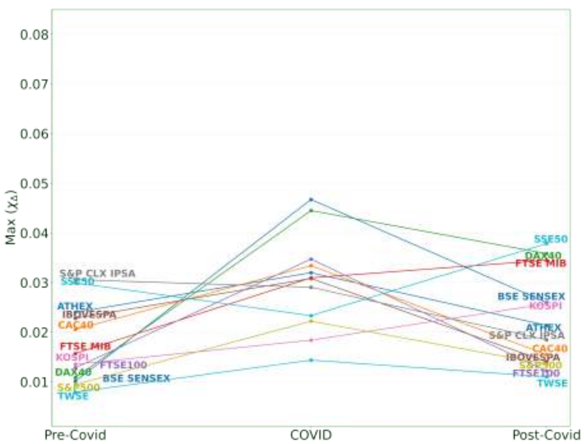


(c) Covid-19 Pandemic

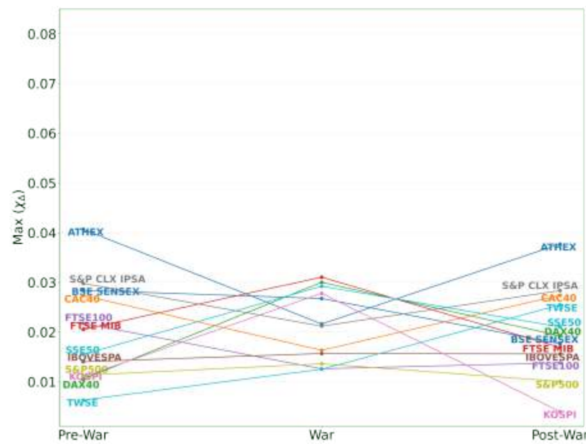


(d) Russia-Ukraine War

Figure 2: Maximum dynamic susceptibility, Max($\chi_\Delta$), for each individual financial market during the pre-crisis, crisis, and post-crisis stages of the four analysed events. The lines track the evolution of structural heterogeneity for specific indices, highlighting the idiosyncratic responses to global shocks.

As shown in Figure 2, the response of the markets followed distinct patterns depending on the nature of the shock. Starting with the 2008 financial crisis (Figure 2(a)), we observe a heterogeneous but broadly consistent response across indices. Prior to the crisis, markets had widely dispersed levels of Max($\chi_\Delta$), with S&P CLX IPSA and SSE50 markets showing notably higher pre-crisis levels of susceptibility. During the crisis period, most markets experienced a sharp increase, with ATHEX, TWSE, and FTSE MIB reaching their highest peaks. Notably, several indices that were relatively stable in the pre-crisis stage, such as FTSE100 and S&P 500, exhibit a strong upward shift, suggesting that the shock propagated across markets regardless of their initial heterogeneity levels.

Reading the European debt crisis (Figure 2(b)), the pattern contrast sharply with the 2008 shock. Rather that exhibiting a generalised increase in susceptibility during the peak of the crisis, most markets experienced a decline in Max($\chi_\Delta$). This reduction was particularly pronounced in TWSE, BSE SENSEX, IBOVESPA, and S&P500, which show the largest drops in susceptibility relative to the pre-crisis stage. This behaviour suggests that, outside Europe, markets were transitioning towards more synchronised dynamics following the dislocations caused by the recent 2008 crisis. In contrast, European markets display more persistent or less pronounced adjustments, reflecting their direct exposure to sovereign debt tensions. Overall, these results support the view that the European debt crisis did not generate a new wave of global fragmentation, but rather represented a regionally concentrated shock, while non-European markets continued a process of structural normalisation.

The pandemic shock (Figure 2(c)) produced a more pronounced and widespread increase in Max($\chi_\Delta$) across all stock markets. BSE SENSEX and DAX40 stand out as the most affected indices, reaching peak values close to 0.047. A key feature of this event is that markets with low pre-crisis susceptibility – particularly among developed economies such as DAX40, BSE SENSEX, and FTSE100 – experienced the largest relative increases, reinforcing the notion that the pandemic disproportionately disrupted the internal structure of more complex and interconnected markets.

In contrast to the global financial crisis and Covid-19 events, the war conflict (Figure 2(d)) produced a markedly subdued response in Max($\chi_\Delta$), but somewhat similarly to the one observed for the European debt shock. The overall level of susceptibility remained low and relatively flat across all markets, with none of them exceeding values of 0.035. FTSE MIB and DAX40 experienced modest increases during the war period, consistent with their geographical proximity to the conflict, while most other indices – particularly those in Asia and the Americas – had little to no change. This pattern suggests that the war acted as a regional rather than a global systemic shock.

This individual market analysis highlights the idiosyncratic nature of each market's response; however, a clearer picture of the aggregate dynamics emerges when markets are grouped by their level of economic development. Thus, Figure 3 presents the evolution of Max($\chi_\Delta$) during the three stages of the selected shocks, aggregating markets in developed and emerging economies.

During the global financial crisis (Figure 3(a)), our results point to a cross-market convergence in structural fragility. While emerging markets exhibited significantly higher baseline heterogeneity in the pre-crisis stage – which reflects their typically higher idiosyncratic risk – both groups converged during the peak of the crisis. This suggests that the 2008 shock acted as a global catalyst for systemic instability, overriding the initial differences in the level of market development.

In Figure 3(b), the European debt crisis reveals a monotonic decline in the values of maximum susceptibility for both groups. Interestingly, emerging markets exhibit the steepest drop from the pre-crisis to the crisis stage. This trend is driven by the performance of major non-European indices such as TWSE, BSE SENSEX, and IBOVESPA (as seen in Figure 2(b)), which experienced a significant structural "cooling off" during this period. The fact that aggregate susceptibility did not spike during the peak of the crisis (2011-–2012) confirms that the European debt crisis was not a global catalyst for price desynchronisation. Instead, while the Eurozone faced internal turmoil, the rest of the global financial system continued to resolve the structural fragmentation inherited from the 2008 global financial crisis, leading to the convergence of both groups at lower levels of heterogeneity in the post-crisis stage.

In contrast, the Covid-19 pandemic (Figure 3(c)) reveals a distinctive pattern where developed markets exhibited higher levels of susceptibility than their emerging counterparts during the crisis period. The steeper slope observed in developed indices suggests that these markets possess a more fragile internal architecture when facing non-financial global shocks. This heightened vulnerability may be attributed to the higher degree of financial integration, algorithmic trading density, and complex cross-asset linkages commonly attributed to mature economies, which can amplify the propagation of exogenous shocks.

Finally, the analysis of the Russia-Ukraine war (Figure 3(d)) confirms what we have already observed: this event was not translated into a global systemic crisis from a price-heterogeneity perspective. Both groups display minimal variation across the three stages, with emerging markets maintaining a slightly higher level of heterogeneity consistent with their long-term baseline. This evidence supports the characterisation of the conflict as a localized geopolitical event with limited impact on the structural stability of global equity markets.

Going beyond the magnitude of market heterogeneity, the analysis of the timescale at which this heterogeneity emerges also provides insightful information. To this end, we examine the characteristic time $\tau_m$, defined as the time lag (in days) at which the dynamic susceptibility reaches its maximum value. This parameter provides a proxy for the speed at which markets incorporate shocks and transition into highly heterogeneous states.

Figure 4 illustrates the evolution of $\tau_m$ for the three stages of the different shocks for each individual stock market. In panel 4(a) – corresponding to the global financial crisis – a generalised downward shift is observed in the response time for all markets. Some indices show significant reductions, moving from horizons of 100-150 days to scales below 50 days, indicating that as the systemic crisis unfolded, the

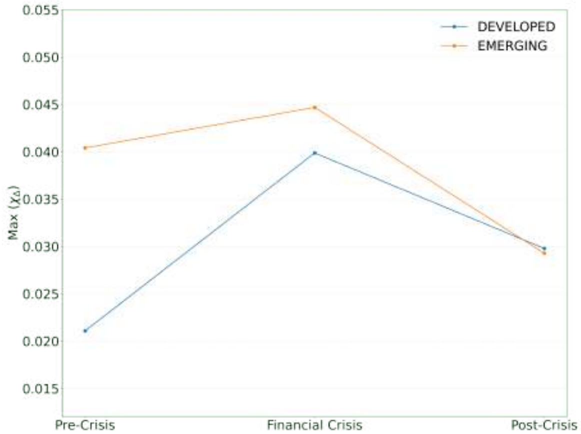


(a) 2008 Global Financial Crisis

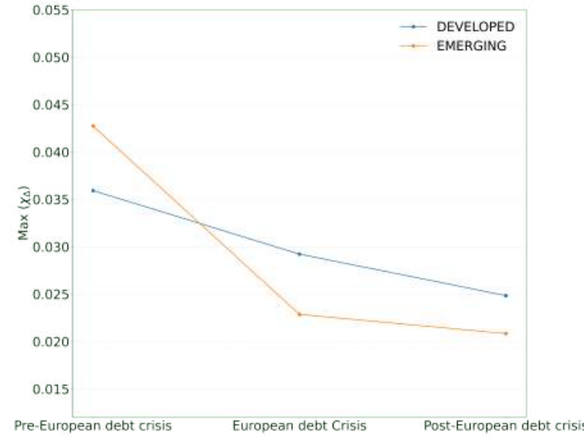


(b) European Debt Crisis

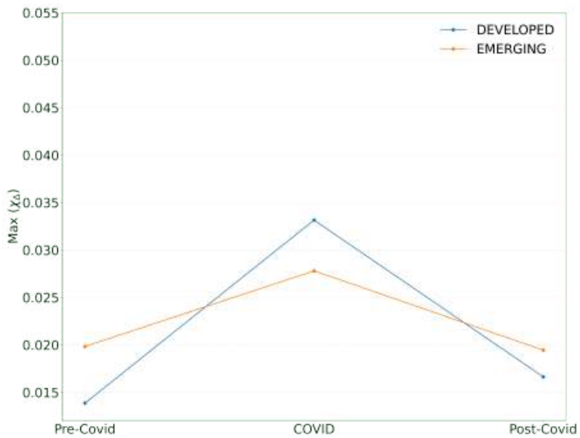


(c) Covid-19 Pandemic

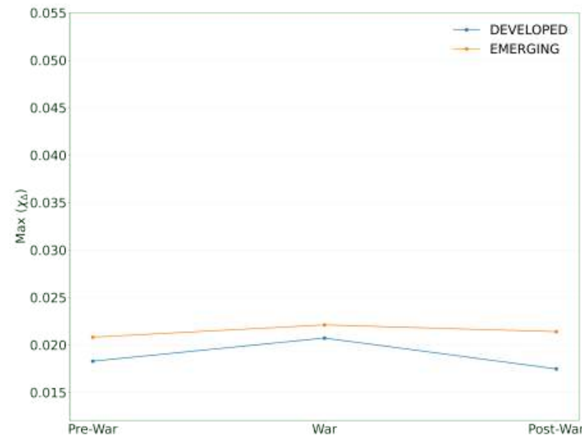


(d) Russia-Ukraine War

Figure 3: Maximum dynamic susceptibility, Max($\chi_\Delta$), differentiating between developed and emerging economies during the pre-crisis, crisis, and post-crisis stages of the four analyzed events. The lines track the evolution of structural heterogeneity for specific indices, highlighting the idiosyncratic responses to global shocks.

internal decoupling of stock prices happened at much faster frequencies.

For the European debt crisis, Figure 4(b) reveals a highly fragmented gobal response. While in the 2008 shock we observed a generalised acceleration of dynamics, this event shows divergent paths: on one hand, DAX40 and TWSE exhibit a significant reduction in $\tau_m$ during the crisis stage, denoting an acceleration of their internal dynamics and faster emergence of price heterogeneity. On the other hand, we identify a group of diverse markets – ATHEX, FTSE 100, SSE 50, and S&P CLX IPSA – that experienced an increase in their characteristic times during the shock. This slowing down of the adjustment process suggests that the extreme uncertainty of the sovereign debt crisis may have led to a state of structural inertia in some indices, where price adjustments became more protracted. This divergent behaviour confirms that the European debt crisis did not impose a uniform temporal signature on global markets, but instead triggered idiosyncratic responses where some systems accelerated while others significantly slowed their internal dynamics.

For the Covid-19 crisis (Figure 4(c)), the acceleration occurred in an even more synchronised way. Most markets, regardless of their pre-pandemic state, converged towards very short values of $\tau_m$.

Finally, for the Russian conflict (Figure 4(d)), it is observed that some of the markets exhibit a decrease in $\tau_m$, while others, – such as SSE50, S&P CLX IPSA, KOSPI or DAX40 – increased their characteristic

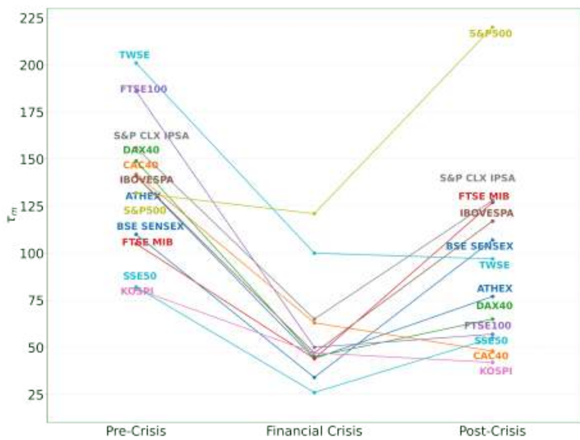


(a) 2008 Global Financial Crisis

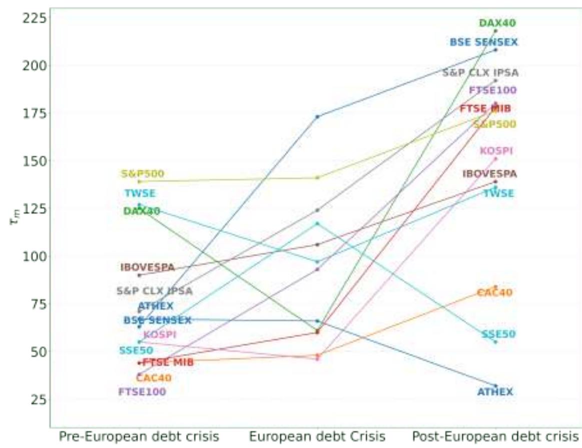


(b) European Debt Crisis

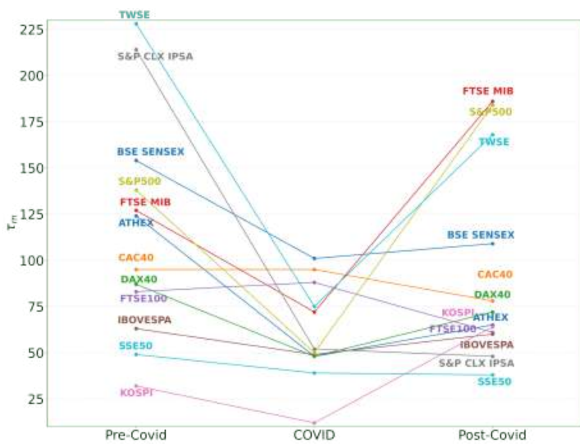


(c) Covid-19 Pandemic

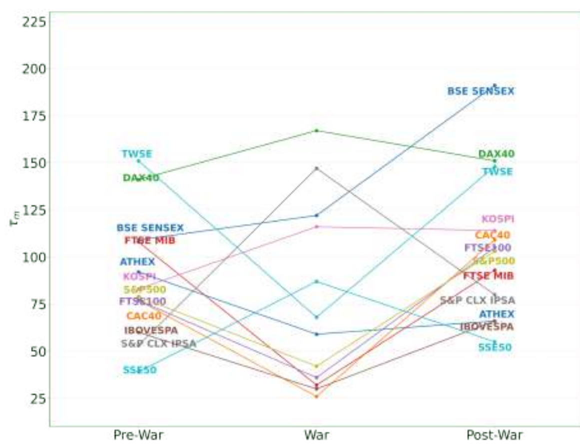


(d) Russia-Ukraine War

Figure 4: Evolution of the characteristic reaction time $\tau_m$ for individual financial markets. Panels (a), (b), and (c) correspond to the 2008 financial crisis, the Covid-19 pandemic, and the Russia-Ukraine War, respectively. $\tau_m$ represents the time lag (in days) at which the dynamic susceptibility reaches its maximum. A decrease in $\tau_m$ during crisis periods indicates an acceleration in market dynamics and a faster emergence of price heterogeneity.

times. This lack of temporal synchronisation confirms that the war did not force a global acceleration of market heterogeneity, in contrast to what we observed for the 2008 and Covid-19 shocks.

Figure 5 presents the evolution of $\tau_m$ when aggregating markets in developed and emerging economies. In this case, a common pattern is observed: periods of crisis are systematically associated with a reduction in $\tau_m$, indicating a faster adjustment of market dynamics under stress.

During the global financial crisis (Figure 5(a)), both groups exhibit a pronounced decrease in their characteristic times, suggesting that the shock accelerated the propagation of information and increased the synchronisation of market responses. However, it is worth mentioning that developed markets presented higher values of $\tau_m$ during the three stages.

For the European debt crisis (Figure 5(b)), the characteristic reaction time reveals a significant temporal divergence. Both groups started from a similar baseline during the pre-crisis stage, but their adjustments followed different trajectories through the shock. Emerging markets exhibited a steady, linear increase in their response time. In contrast, developed markets remained almost stable during the crisis itself, only to undergo a drastic increase in the post-crisis stage, reaching values near 170 days. This pattern suggests that developed economies experienced a much more severe structural slowdown in the


(a) 2008 Global Financial Crisis

(b) European Debt Crisis

(c) Covid-19 Pandemic

(d) Russia-Ukraine War

Figure 5: Evolution of the characteristic reaction time $\tau_m$ differentiating between developed and emerging markets. Panels (a), (b), (c), and (d) correspond to the 2008 financial crisis, the European debt crisis, the Covid-19 pandemic, and the Russia-Ukraine War, respectively. $\tau_m$ represents the time lag (in days) at which the dynamic susceptibility reaches its maximum. A decrease in $\tau_m$ during crisis periods indicates an acceleration in market dynamics and a faster emergence of price heterogeneity.

aftermath of the crisis, ending the period as significantly slower systems than their emerging counterparts.

The pandemic shock reinforces the pattern observed in Figure 5(a), with a sharp decline in $\tau_m$ for both groups, as observed in Figure 5(c). However, in contrast to the financial crisis, developed markets in this crisis display a more pronounced drop, indicating a faster transition into states of high heterogeneity. This result complements the findings from the susceptibility analysis, suggesting that not only were developed markets more fragmented during the pandemic, but they also reached this state more rapidly.

Finally, on panel 5(d), it can be observed that the Russia-Ukraine conflict did not produce a comparable acceleration in the market dynamics for both groups. While developed markets experienced a reduction in $\tau_m$, the magnitude of the change is smaller than in the two previous crises. Moreover, emerging economies remained relatively stable, exhibiting a more gradual increase and adjustment process. These results further support the fact that the war was a localised shock with limited impact on the global temporal structure of market dynamics.

Overall, these results highlight that major systemic crises are characterised not only by increased heterogeneity but also by a compression of the timescales over which market adjustments take place.

The static analysis performed so far confirms that global shocks produce alterations in both the magnitude and the speed of market heterogeneity. Nonetheless, the use of fixed windows limits the analysis and the ability to identify the precise moment at which the transition to the crisis is produced or to detect early-warning signals. To overcome this and with the aim of providing a continuous longitudinal monitoring of market stability, we implement a rolling window analysis, presented in the following Subsection 3.1.

### 3.1 Rolling window analysis

To investigate the temporal evolution of market heterogeneity, we implement a rolling window approach as described in Section 2.2. For each window, we compute the dynamic susceptibility $\chi_\Delta(\tau)$ and extract both its maximum value and the associated characteristic time $\tau_m$. The experiment is performed for three different cases: (a) considering markets individually, (b) grouping markets in terms of their economic development (developed and emerging markets), and (c) grouping markets by geographic regions (Europe, Asia, and America).

Given that the analysis depends on the choice of the threshold $\Delta$, we consider a range of values $\Delta = 0.02, 0.04, 0.06, 0.08, 0.10, 0.12, 0.14, 0.16, 0.18, 0.20$. For clarity of exposition, the main results are presented for $\Delta = 0.16$ in Figure 6, which provides a representative balance between short-term fluctuations and persistent structural changes. The results for the alternative values of $\Delta$ are reported in Appendix B and confirm the robustness of our findings.

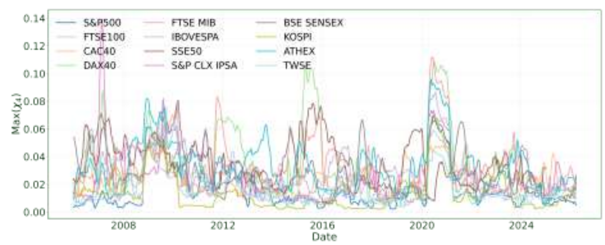


(a) Individual markets susceptibility

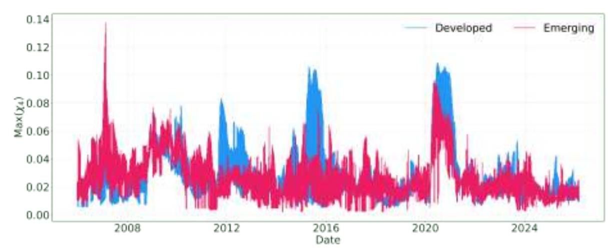


(b) Developed vs. Emerging markets

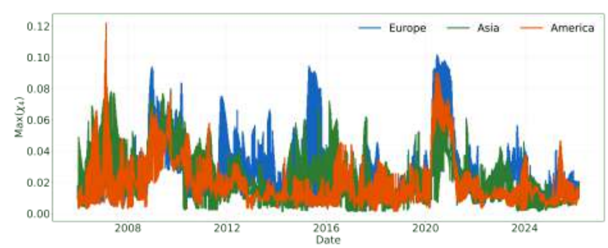


(c) Regional aggregation

Figure 6: Evolution of maximum dynamic susceptibility Max($\chi_\Delta$) using a rolling window for $\Delta = 0.16$. The top panel (a) displays the idiosyncratic paths of the twelve analyzed markets. The bottom panels show aggregate dynamics by economic development (b) and geographic region (c).

Figure 6(a) reveals that peak susceptibility is not only associated with well-known global crises, but also with localized periods of volatility. For instance, the 2008 financial crisis is preceded by a gradual rise in Max($\chi_\Delta$) starting in late 2007. This lead–lag relationship suggests that the considered fragmentation measure captures the build-up of structural imbalances before they materialize as a full-scale price collapse, offering a clear advantage over traditional lagging indicators of risk. In contrast, the Covid-19 shock in early 2020 exhibits a significantly steeper and more synchronized spike across all markets, generating a distinct fragmentation regime characterized by rapid and coordinated structural dislocation.

The aggregate analysis by economic development (Figure 6(b)) reveals an important structural shift. During the financial crisis, the emerging markets group reached the highest absolute peak of susceptibility. Conversely, during the pandemic, developed markets exhibited a more persistent and intense level of heterogeneity. This pattern suggests a shift in the nature of systemic risk: developed financial systems, while efficient under normal conditions, may be more vulnerable to structural fragmentation during non-conventional crises. This heightened vulnerability may be linked to higher levels of financial integration and the widespread use of algorithmic and high-frequency trading, which can amplify the propagation of shocks.

Finally, the regional aggregation (Figure 6(c)) highlights the geographic dimension of contagion. During the Eurozone debt crisis – which spanned the period 2011–2012 – Europe experienced a distinct and prolonged phase of elevated susceptibility that was less pronounced in the American and Asian regions. Similarly, the 2020 pandemic led to an almost simultaneous synchronisation across all regions. In contrast, the post-2022 period, marked by the Russia–Ukraine war, primarily affected European markets and, to a lesser extent, American ones. This pattern reinforces the view that geopolitical shocks tend to remain regionally contained, in contrast to the global impact of financial or pandemic-driven crises.

From a financial perspective, these rolling-window results indicate that $\mathrm{Max}(\chi_\Delta)$ can be interpreted as a proxy for market fragmentation and structural dislocation. Periods of elevated fragmentation correspond to a breakdown in the synchronous behaviour of assets, where different segments of the market adjust at different speeds. This loss of coherence has direct implications for risk management, as it undermines the assumptions of stable correlations and effective diversification.

# 4 Conclusions

# References

Molero-González, L., Trinidad-Segovia, J. E., Sánchez-Granero, M. A., Clara-Rahola, J., and Puertas, A. M. (2025). Dynamic heterogeneities in stock markets. *Physica A: Statistical Mechanics and its Applications*, 669:130567.

# A Descriptive Statistics

Table 2 presents the main descriptive statistics of the logarithm of the close prices for the 12 analysed equity markets. We denote by $p$ the number of stocks within each market, and by $n$ the number of observations (trading days).

Table 2: Descriptive statistics of the logarithm of the close prices for the analyzed markets. $p$ denotes the number of stocks, $n$ the number of trading days.

| | S&P500 | FTSE 100 | CAC40 | DAX40 | FTSE MIB | IBOVESPA | SSE50 | S&P CLX IPSA | BSE SENSEX | KOSPI | ATHEX | TWSE |
|---|---|---|---|---|---|---|---|---|---|---|---|---|
| $p$ | 400 | 31 | 14 | 29 | 27 | 30 | 22 | 20 | 26 | 378 | 41 | 32 |
| $n$ | 5322 | 5322 | 5458 | 5380 | 5378 | 5262 | 4874 | 5306 | 5218 | 5237 | 5298 | 5198 |
| Mean | 3.7424 | 2.5279 | 3.0648 | 3.6748 | 1.7645 | 2.2734 | 2.3630 | 6.5156 | 5.5254 | 9.0341 | 1.0748 | 3.5109 |
| Std | 1.0956 | 1.1666 | 2.2354 | 1.0275 | 1.7007 | 1.6087 | 1.4202 | 1.8092 | 1.9883 | 1.6853 | 2.2004 | 1.3188 |
| Min | -2.0479 | -0.9999 | -9.2103 | -1.2557 | -1.8257 | -3.3393 | -1.0587 | 1.5260 | -13.5256 | 3.6949 | -2.9800 | 0.4141 |
| 25% | 3.0343 | 1.7322 | 1.8795 | 3.0053 | 0.7432 | 1.5110 | 1.4030 | 5.1571 | 4.5357 | 7.8430 | -0.1054 | 2.5486 |
| 50% | 3.7028 | 2.5193 | 2.7190 | 3.7043 | 1.6232 | 2.1138 | 2.3530 | 6.7554 | 5.7513 | 8.8459 | 0.8733 | 3.4141 |
| 75% | 4.4397 | 3.4006 | 3.9560 | 4.3750 | 2.3957 | 2.7795 | 3.1522 | 7.8759 | 6.7381 | 10.0841 | 1.7000 | 4.2929 |
| Max | 9.2028 | 5.4528 | 12.3429 | 7.5951 | 12.0629 | 15.0102 | 7.7682 | 11.5321 | 9.7582 | 22.6733 | 15.2497 | 8.4414 |
| Skewness | 0.0237 | -0.0552 | 0.5637 | -0.1015 | 2.5371 | 2.9660 | 0.5637 | -0.2294 | -2.6691 | 0.8312 | 3.0497 | 0.7425 |

# B Rolling window experiment

This appendix reports the rolling-window estimates of $\mathrm{Max}(\chi_\Delta)$ for alternative threshold values, excluding the benchmark case of $\Delta = 0.16$ presented in the main text. The figures confirm that the main patterns discussed in the paper are qualitatively robust across a broad range of threshold specifications.

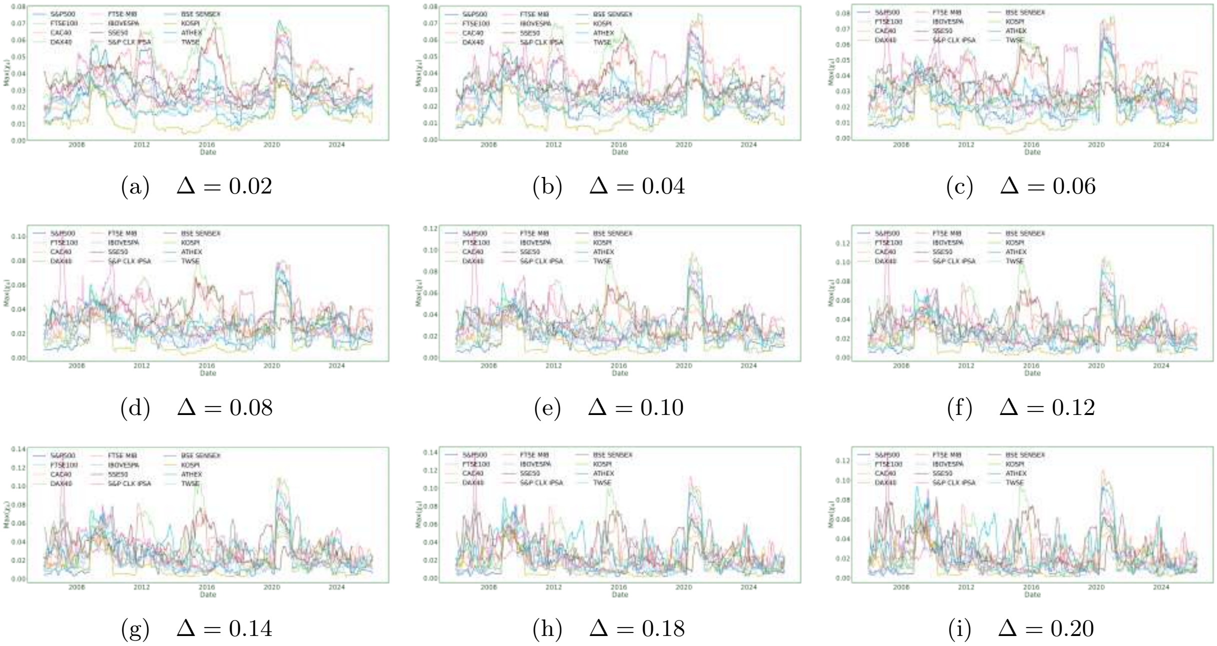


(a) $\Delta = 0.02$ (b) $\Delta = 0.04$ (c) $\Delta = 0.06$

(d) $\Delta = 0.08$ (e) $\Delta = 0.10$ (f) $\Delta = 0.12$

(g) $\Delta = 0.14$ (h) $\Delta = 0.18$ (i) $\Delta = 0.20$

Figure 7: Rolling-window estimates of $\mathrm{Max}(\chi_\Delta)$ for individual markets under alternative threshold values $\Delta$. The main text reports results for $\Delta = 0.16$; the remaining thresholds are shown here as a robustness check.

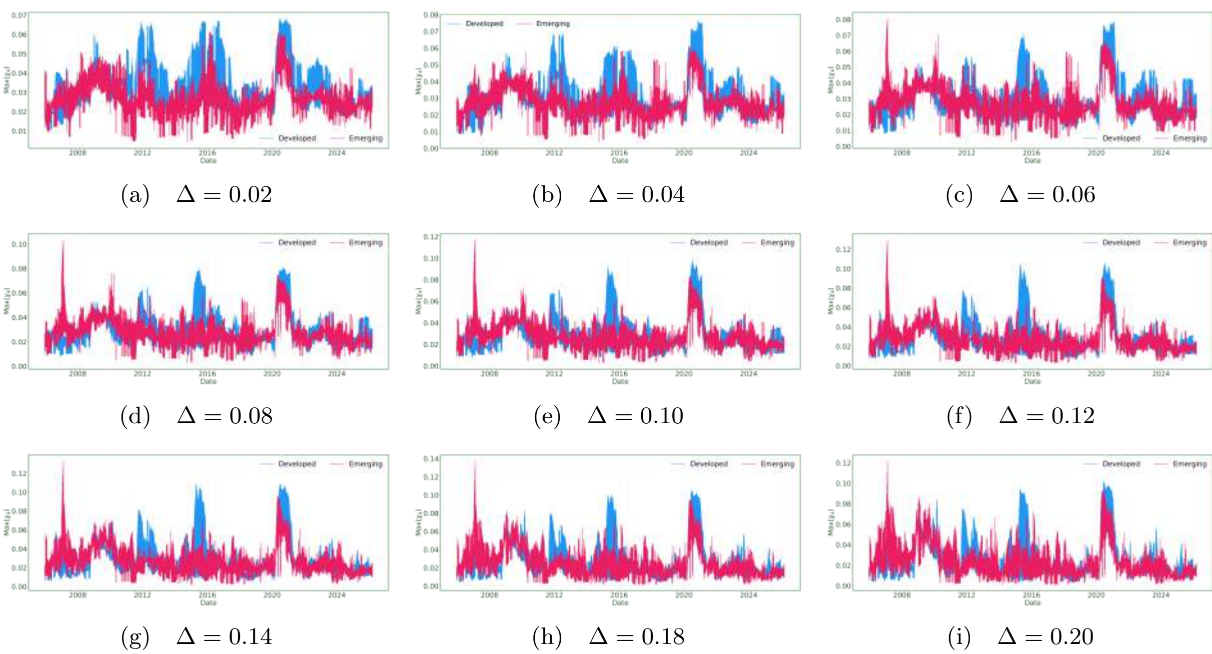


(a) $\Delta = 0.02$ (b) $\Delta = 0.04$ (c) $\Delta = 0.06$

(d) $\Delta = 0.08$ (e) $\Delta = 0.10$ (f) $\Delta = 0.12$

(g) $\Delta = 0.14$ (h) $\Delta = 0.18$ (i) $\Delta = 0.20$

Figure 8: Rolling-window estimates of $\mathrm{Max}(\chi_\Delta)$aggregated by level of economic development under alternative threshold values $\Delta$. The main text reports results for $\Delta = 0.16$; the remaining thresholds are shown here as a robustness check.

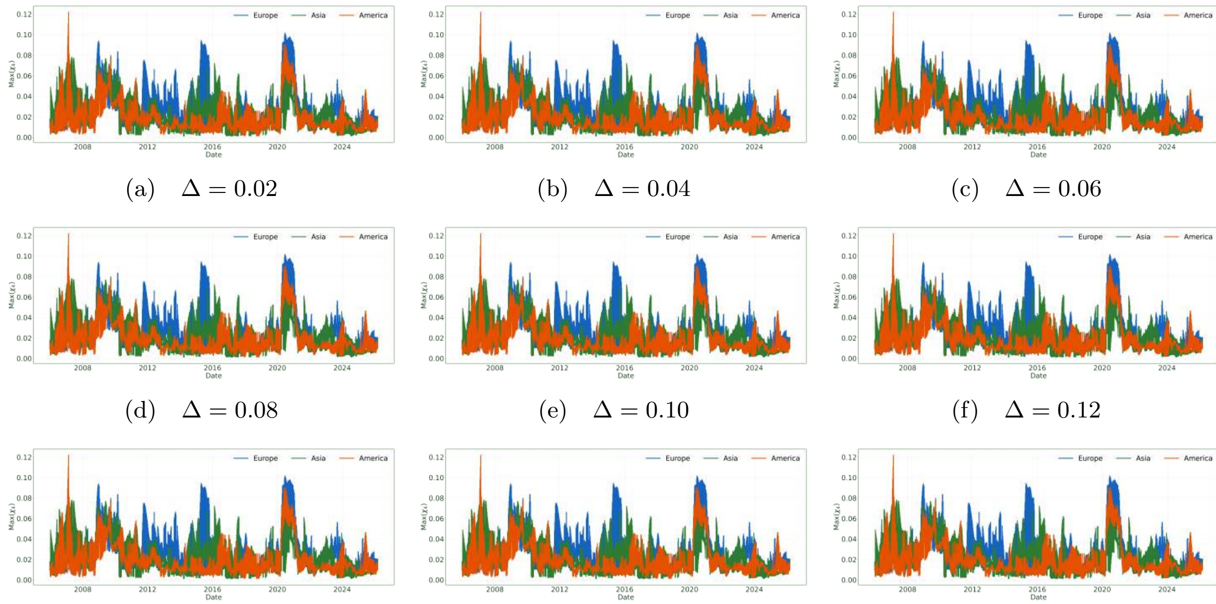


(a) $\Delta = 0.02$ (b) $\Delta = 0.04$ (c) $\Delta = 0.06$

(d) $\Delta = 0.08$ (e) $\Delta = 0.10$ (f) $\Delta = 0.12$

(g) $\Delta = 0.14$ (h) $\Delta = 0.18$ (i) $\Delta = 0.20$

Figure 9: Rolling-window estimates of Max($\chi_\Delta$)aggregated by geographic region under alternative threshold values $\Delta$. The main text reports results for $\Delta = 0.16$; the remaining thresholds are shown here as a robustness check.

# C Correlation with benchmark indicators

Table 3 provides the full correlation results between the peak of dynamical susceptibility ($\chi^*_\Delta$, for $\Delta = 0.16$) and three standard financial benchmarks: equally-weighted realized volatility ($\sigma_{vol}$), average pairwise correlation ($\bar{\rho}$), and the first eigenvalue ratio from PCA ($\lambda_1/N$).

Table 3: Pearson correlation coefficients between the peak dynamical susceptibility ($\chi^*$) and standard financial benchmarks for the rolling window analysis.

| **Market** | **Corr**$(\chi^*, \sigma)$ | **Corr**$(\chi^*, \bar{\rho})$ | **Corr**$(\chi^*, \lambda_1/p)$ |
|---|---|---|---|
| KOSPI | 0.841 | 0.828 | 0.823 |
| S&P 500 | 0.844 | 0.711 | 0.710 |
| FTSE 100 | 0.744 | 0.694 | 0.700 |
| IBOVESPA | 0.654 | 0.681 | 0.739 |
| TWSE | 0.751 | 0.659 | 0.666 |
| DAX 40 | 0.603 | 0.598 | 0.609 |
| ATHEX | 0.512 | 0.554 | 0.551 |
| FTSE MIB | 0.633 | 0.526 | 0.520 |
| S&P CLX IPSA | 0.509 | 0.488 | 0.496 |
| BSE SENSEX | 0.599 | 0.460 | 0.456 |
| SSE 50 | 0.587 | 0.420 | 0.426 |
| CAC 40 | 0.429 | 0.380 | 0.374 |